Indian Journal of Pure & Applied Physics
Vol. 57, July 2019, pp. 483-491

The simultaneous effects of the wetting layer, intense laser and the conduction band non-parabolicity on the donor binding energy in a InAs/GaAs conical quantum dot using the numerical FEM

Ahmed Sali[a,*], Abdellah Rezzouk[a], Najia Es-Sbai[b] & Mohammed Ouazzani Jamil[c]

[a]Department of Physics, Faculty of Science, Sidi Mohamed Ben Abdellah University, B.P.1796 Dhar El Mahraz, Fez, Morocco
[b]Faculty of Science and Techniques, Sidi Mohammed Ben Abdellah University, B.P. 2202, Route d'Imouzzer, Fez, Morocco
[c]Université privée de Fès, Lotissement Quaraouiyine, Route d'Ain Chkef 30000, Fès Morocco

Received 10 January 2018; accepted 12 March 2019

Using the finite element method, we have performed a systematic study on the ground-state binding energy (E_b) of a donor impurity confined in a InAs/GaAs conical quantum dot (CQD) with wetting layer (WL) and a realistic finite confining potential. The simultaneous effect of the applied electric and magnetic fields as well as the influence of an intense laser field have been performed on the E_b within the effective mass approximation. The band non-parabolicity effect is also considered using the energy dependent effective mass approximation. It has been shown that the E_b is highly dependent on the internal and external CQD structure parameters such as radial thickness, height and WL thickness, external electric, magnetic fields and intense laser field. The results we have obtained show that a quite significant contribution of the WL effects on the ground state energy and the E_b has found at small values of the cone radius. In the low confinement regime, the effect of the conduction band non-parabolicity becomes gradually smaller as the value of the cone radius increases and the influence of high-frequency laser increases with the non-parabolicity effect in the regime of small QD radius. Our results are in good agreement with those obtained in the literature.

Keywords: FEM, Quantum dot, Wetting layer, Binding energy, Conduction band non-parabolicity

1 Introduction

Semiconductor nanostructures have attracted lots of research interest in the past few years due to their unique physical properties and their wide quantum functional device applications in micro – and optoelectronic devices. The ultimate limit of low dimensional structures is the quantum dot (QD), in which the carriers are confined in all three directions, thus reducing the degrees of freedom to zero**.** Therefore, the energy levels of electrons in such QDs are fully quantized as in an atom. As these QDs contain relatively small number of atoms, their electronic and optical properties depend strongly on the size, stoichiometry, and shape. Quasi-zero dimensional systems, especially self-assembled quantum dots (SAQDs) have been a subject of numerous investigations owing to their promising potential application in optoelectronic devices, quantum computing, information storage, and electrical metrology[1-3]. SAQDs can be manufactured during Stranski–Krastanow growth method in process of epitaxy of hetero-structures with large lattice mismatch between the substrate and the active layer[4]. Semiconductor nanostructures based on III–V group elements are well known and widely investigated in the past[5]. Among them, InAs QDs grown on GaAs substrates using molecular beam epitaxy are the most commonly studied system and one of the first well established technologically and extensively explored for applications in optoelectronic devices such as QDs lasers[6], light emitters and detectors[7,8], optical amplifiers or novel quantum devices like single photon sources[9]. In the archetype InAs/GaAs QD system, the formation of dots is associated with the relatively large 7% lattice mismatch. When deposited on GaAs, the InAs initially forms a two dimensional (2D) planar layer and strain builds up in the layer until the thickness reaches a critical value. In literature, the 2D layer is called the wetting layer (WL) since it wets the GaAs substrate due to higher surface energy of GaAs than that of InAs. As the WL exceeds a critical thickness, the growth mode switches from 2D to 3D leading to the formation of a SAQD on the top of the WL[10]. The critical thickness

*Corresponding author (E-mail: sali_ahm@hotmail.com)

of the WL depends on materials used and fabrication techniques[11].

Although SAQD is grown on top of the WL, many works concentrating on the electronic and optical properties of InAs/GaAs SAQDs have been studied disregarding the effect of WL and its role[12-16]. This ignorance in theoretical works may arise from mathematical complexities in making analytical models. The first theoretical study of the electronic properties of these structures has used the single-band effective-mass theory to calculate the energy levels and wave functions in InAs/GaAs cone-shaped QDs[12]. Experimentally; it has been shown that the SAQDs cannot be grown without WL[17]. In fact, the coupling between electronic states in the QD and WL is essential to achieve better results[18,19].

Stimulated by the rapid progress in nanometer-scale fabrication technology, a large number of papers focused on the electronic and optical properties of InAs/GaAs SAQDs systems of different shapes with WL effects has been published using different methods[19-24].

The study of impurity states in semiconductor QDs is imperative as the addition of impurities can change the properties of any quantum device dramatically since the confinement in all three direction, increases greatly the Coulomb interaction. The introduction of impurities in QDs and particularly in SAQDs is therefore of fundamental importance for a deep understanding of their effects on electronic and optical properties. However, the above significant number of studies were devoted to the investigation of WL effect relative only to the charge carriers, but there exist very few studies regarding the effect of donor impurities on the optical and electronic properties in InAs/GaAs QDs with WL[25].

Nanoelectronics is a promising area that has drawn considerable interest due to the possibilities it opens in applied physics[26]. As it is well known, the application of either an electric or a magnetic field, among other external perturbations, changes the quantum states of carriers confined in nanostructures[27]. Application of an electric field in the growth direction of the system causes polarization of carrier distribution and shifts the quantum energy states. These effects cause considerable changes in the energy spectrum of the carriers, which may be used to control and modulate the intensity output of devices[28]. Moreover, the presence of a uniform magnetic field causes a second magnetic confinement of the charges which superposes its geometric counterpart; this yields an increment of the binding energy due to the reductions in the radius of the cyclotron orbits with the applied field[29].

In addition to the simple geometries that can QDs have like spherical and cylindrical, QDs can be fabricated with more complex geometry such as pyramidal, lens-shaped and cone-like where their theoretical treatment within the traditional quantum mechanical approach is mathematically difficult[30-32]. The understanding of the effects of external electromagnetic fields on the electronic and optical properties of complexes QDs is of a primordial interest for the evolution of such research area. However, the literature is sparse with studies on the electric and magnetic fields dependence of binding energy in these complexes systems[33-36]. The ground state of impurity confined by a GaAs pyramid shaped QD as well as the diamagnetic shift of the impurity energy have been investigated under the combined effect of magnetic field and the hydrostatic pressure using a variational method within the effective mass approximation[33]. In lens-shaped QDs, the effect of an external magnetic field on the energy levels, wave functions and the optical properties such as the second harmonic generation and third-harmonic generation has been determined using the finite element method (FEM)[34]. In a more recent work, Niculescu *et al*.[35] studied the energy levels for the ground state and first excited states and optical properties of an electron inside the GaAs pyramidal-shaped QDs under the combined action of the electric and magnetic fields applied in the growth direction within the density matrix formalism with the use of the effective mass and parabolic band approximations. Aderras *et al*.[36] presented very recently a calculation of stark effect and the polarizability of shallow-donor impurity located in the centre of lens shaped QD by a variational method and in the effective-mass approximation using an infinite hard-wall confining potential to describe the barriers at the dot boundaries.

Besides the external magnetic and electric effects discussed above, special attention has recently been given to the laser interaction with semiconductor heterostructures. A number of experimental and theoretical investigations have been concerned with the quantitative understanding of laser field effects on the electronic and optical properties of low dimensional semiconductor heterostructures[37], a subject of paramount importance for one interested in

the design of new optoelectronic devices. However, there has been little interest in the study of intense laser–field radiation effects on the optical and the electrical properties of impurities in complexes SAQDs[38]. Within the effective mass approximation, Niculescu has examined the binding energy and photoionization cross section of a donor impurity in a pyramid shaped QD under simultaneous effects of the hydrostatic pressure and high-frequency laser field[38]. Their results showed that the electronic and optical properties depend on the donor position, laser field intensity and pressure.

Among the complexes QDs mentioned above, more attention had been paid to the cone-shaped QDs since they have shown remarkable potential for prospective applications in the fields of optoelectronics and quantum information, in devices such as QD LED and single photon sources[39-42]. The electronic and optical properties of CQD in the absence of impurity have been extensively studied in the past[12,21,39,43-46]. On the contrary, few works concentrating on the donor impurity in the absence and presence of the exterior perturbations such as the electric and magnetic fields have been established in CQD structures[47-50].

It is worth remarking that due to the complicated shapes of CQD, the calculations of energy levels, wave functions and the donor binding energy is a nontrivial task, which requires considerable theoretical effort. To obtain an analytical solution of the problem of a hydrogenic donor impurity confined in a QD of complex realistic geometry like CQD and including the effects of the surrounding media is not possible in general by using common standard methods. The finite value of the potential barrier could be a fundamental parameter when considering different external factors such as the magnetic, electric and laser radiation fields or when including others physical effect, such as the WL in a QD. We therefore use the FEM to solve the Schrödinger equation associated with the problem of an impurity in a CQD with a finite confinement potential. Since it yields accurate Eigen energy and Eigen states of one-, two- and three dimensional structures of arbitrary shape, but it is very computationally intensive[51-53]. The most above developed calculations in CQD in the presence of impurities were done within only the simple parabolic band approximation for the electron effective mass. On the other hand, it is well known that energy dispersion relation is only parabolic around band edge. So, in a more realistic model, in order to provide more accurate results of the energy levels and the donor binding energy, it is necessary to take into account the non-parabolicity of conduction band[54,55].

We know that the cone shaped QDs have been investigated theoretically and experimentally. The donor binding energy in a CQD with WL under the simultaneous action of a static magnetic and electric fields and under an external laser radiation field has not been investigated so far. Therefore, in the present work, we calculate the energy of the ground state of a CQD with finite potential barrier height as well as the binding energy of an on-center shallow donor impurity as a function of the of the radius, the height of the CQD, the WL thickness and the laser field intensity under the combined effect of electric and magnetic fields. The calculations are made with and without taking into account the band-non parabolicity using the effective mass approximation and the numerical FEM.

2 Basic Theory

We consider in Fig. 1 (a) a schematic view of the conical InAs QD buried in a GaAs matrix with cylindrical symmetry. The WL is modeled by a monolayer-thick InAs layer at the base of the cone. The origin of the z-axis is taken at the centre of the structure. H denotes the height of the CQD, r is base radius and L is the WL thickness. The geometry has symmetrical axis so only half part has been considered in this study as shown in Fig. 2 (b). Within the effective mass and parabolic-band approximation, the interaction of an electron with a hydrogenic donor impurity confined in a InAs/GaAs CQD, in the

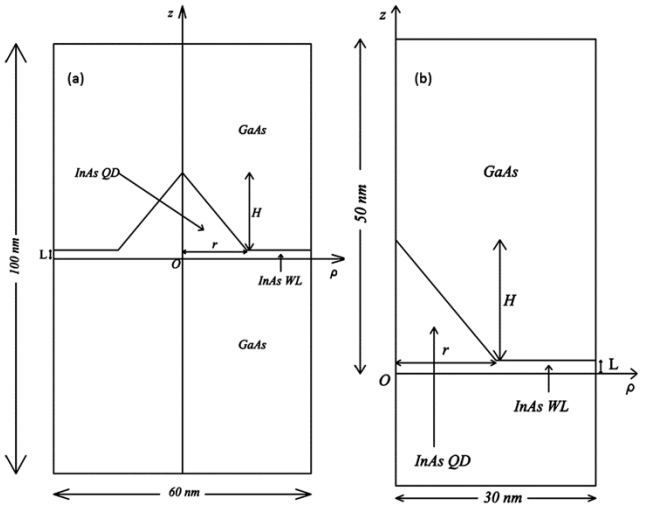

Fig. 1 – Schematic representation of conical shaped InAs QD with WL embedded in a GaAs matrix.

presence of external magnetic field B and electric field F applied along the z axis and intense high-frequency laser field polarized along the z direction is described by the Hamiltonian:

$$\mathscr{H} = -\frac{\hbar^2}{2m^*_{d,b}}\left(\frac{\partial^2}{\partial\rho^2}+\frac{1}{\rho}\frac{\partial}{\partial\rho}+\frac{\partial^2}{\partial z^2}+\frac{1}{\rho^2}\frac{\partial^2}{\partial\theta^2}\right) + \frac{e\hbar B}{2m^*_{d,b}c}l_z + \frac{e^2}{8m^*_{d,b}c^2}B^2\rho^2 + |e|Fz \quad \ldots(1) + V(\rho,z,\alpha_0) + V_c(\rho,z) \qquad \ldots(1)$$

Where $\hbar$ is the reduced Plank constant, the two subscripts d and b in $m^*_{d,b}$ refer to the InAs QD and the GaAs barrier layer materials, respectively. $m^*_d(m^*_b)$ is the electron effective mass of the InAs(GaAs) CQD. The ρ (z) coordinate gives the relative separation of the electron from the impurity ion along (perpendicular to) the CQD radial direction. The second term of Eq. (1) represents the interaction between the external magnetic field B applied along the z direction and the orbital angular momentum l, the third diamagnetic term is the magnetic field induced confinement potential and the fourth term describes the interaction between the electron and the external electric field assumed to be in the z direction.

The last term of Eq. (1) represents the laser-dressed Coulomb interaction between the electron and the impurity ion located at the position $r_0 = (\rho_0, z_0)$. To describe the impurity atom behavior in the presence of the laser field, we assume the system to be under the action of laser radiation represented by a monochromatic plane wave. The laser beam is non-resonant with the semiconductor structure, and linearly polarized perpendicular to the dot radial direction, chosen as z-axis. Following the approach of Ehlotzky[56], in the high-frequency limit, the electron sees a laser dressed potential:

$$V(\rho,z,\alpha_0) = -\frac{e^2}{8\pi\varepsilon_{d,b}\varepsilon_0}\left[\frac{1}{\sqrt{(\rho-\rho_0)^2+(z-z_0+\alpha_0)^2}}+\frac{1}{\sqrt{(\rho-\rho_0)^2+(z-z_0-\alpha_0)^2}}\right] \qquad \ldots(2)$$

Where ε_d (ε_b) is the static dielectric constant of the InAs (GaAs) CQD. ε_0 is the permittivity of free space and α_0 is the laser dressing parameter given by:

$$\alpha_0 = \frac{eA_0}{m^*_{d,b}c\omega_L} \qquad \ldots(3)$$

in which e, c, A_0 and ω_L are the charge of the electron, velocity of the light, the amplitude of the vector potential and the frequency of applied field, respectively.

Taking into account the appreciable extent of the wavefunction outside the dot, we neglect the laser dressing effect on the confinement potential. Due to the weak confinement regime associated with even mirror boundary conditions, it is expected this "one-effect" approach[38,57] to be a reasonable approximation.

The spatial confinement potential energy which confines the donor electron is given by:

$$V_c(\rho,z) = \begin{cases} 0, (\rho,z)\ \epsilon\ \text{material InAs} \\ V_0, (\rho,z)\ \epsilon\ \text{material GaAs} \end{cases} \qquad \ldots(4)$$

with $V_0 = Q_c\,\Delta E_g^{\Gamma}$ is the barrier height, $Q_c = 0.7$ is the conducting band offset parameter[58,59] and $\Delta E_g^{\Gamma} = E_g(\text{GaAs}) - E_g(\text{InAs})$ stands for the total energy gap difference between the InAs dot and the GaAs barrier medium at the Γ point.

The Eigen function of the electron associated to the Hamiltonian (Eq. 1) can be described by the governing one-band Schrödinger equation which, in cylindrical coordinates becomes:

$$H\,\psi(\rho,z,\theta) = E\ \psi(\rho,z,\theta) \qquad \ldots(5)$$

Where E is its unknown energy eigenvalue..

The use of cylindrical symmetry allows us to consider that the wave function is separable on:

$$\psi(\rho,z,\theta) = \chi(\rho,z)\varphi(\theta) \qquad \ldots(6)$$

The envelope function φ satisfies the equation: $\frac{1}{\varphi(\theta)}\frac{\partial^2\varphi(\theta)}{\partial\theta^2} = -n^2$ which gives as solution: $\varphi(\theta) \propto e^{in\theta}$ with $\varphi(\theta+2\pi) = \varphi(\theta)$ and $n = 0, \pm1, \pm2, \ldots$ is the electron orbital quantum number.

After straightforward simplification process, the remaining part of (Eq. 1) can be written as:

$$-\frac{\hbar^2}{2m^*_{d,b}}\left(\frac{\partial^2\chi_n(\rho,z)}{\partial\rho^2}+\frac{1}{\rho}\frac{\partial\chi_n(\rho,z)}{\partial\rho}+\frac{\partial^2\chi_n(\rho,z)}{\partial z^2}\right) + \frac{\hbar^2}{2m^*_{d,b}}\frac{n^2}{\rho^2}\chi_n(\rho,z) + \frac{e\hbar B}{2m^*_{d,b}c}l_z\chi_n(\rho,z) + \frac{e^2}{8m^*_{d,b}c^2}B^2\rho^2\chi_n(\rho,z) + |e|Fz\chi_n(\rho,z) + V_c\chi_n(\rho,z) + V(\rho,z,\alpha_0)\chi_n(\rho,z) = E_n\chi_n(\rho,z) \qquad \ldots(7)$$

Since we expect significant effect of spin-orbit splitting in narrow gap III-V semiconductors, it is very interesting to take into consideration the non-parabolicity for the electron's dispersion relation for which the effective mass is given as [54,55]:

$$m_{np}^{*} = \frac{m_{d,b}^{*}\left(E_g + \frac{2\Delta}{3}\right)}{E_g\left(E_g + \Delta\right)} \frac{\left(E_g + E\right)\left(E_g + E + \Delta\right)}{\left(E_g + E + E_g + \frac{2\Delta}{3}\right)} \quad \ldots (8)$$

Where E_g is the energy band gap between the valence band and the conduction band, Δ is the spin-orbit splitting energy and E is the electron energy.

Since it's impossible to give an analytical solution to the Eq. (7) due to the presence of the impurity Coulombic potential and due to the complexity of the structure geometry with the use of a finite confinement potential, we therefore solve this equation by using the FEM which converges to the exact solution. The calculations have been done using the Dirichlet boundary conditions that have been applied for the external boundaries where the wave function should vanish and Newman condition to the internal boundary ensuring the continuity of the wave function. More details on the calculation procedure can be found elsewhere[21].

In all what follows, we assume a single donor impurity located at the center of the CQD (i.e., $\rho_0 = 0$ and $z_0 = 0$) and we limited our study to the donor ground state level ($n = 0$ and $l_z = 0$).

The donor binding energy E_b of the ground state is obtained from the usual definition:

$$E_b = E_{sub} - E_0, \quad \ldots (9)$$

Where E_{sub} is the Eigen value solution of Eq. (1) without the impurity Columbic potential term and E_0 is the ground state energy with the impurity.

3 Results and Discussion

Our numerical simulations of the energy levels and the donor binding energy as a function of the external and internal parameters are carried out for InAs/GaAs CQD. Because the CQD with its WL has not a regular and simple geometry, the numerical calculations were done using the FEM. The physical parameters pertaining to this system are[20,60]: $m_e^* = 0.023\ m_0$, $E_g = 0.42$ eV, $\varepsilon = 15.2$, $\Delta = 0.48$ eV for InAs and $m_e^* = 0.0665\ m_0$, $E_g = 1.519$ eV, $\varepsilon = 12.5$, $\Delta = 0.34$ eV for GaAs. In what follows the energy unit is expressed in meV, the length unit is nm, the unit of strength of electric field is KV/cm and γ is a dimensionless measure of the magnetic field.

Figures 2 and 3 display, respectively, the variation of the impurity donor binding energy and the electron ground state energy as a function of the base radius of the *InAs*/GaAs conical shaped QD for three values of the WL thickness $L = 1$ nm (solid line), $L = 2$ nm. (dashed line) and $L = 3$ nm (dotted line) and for a fixed value of the cone height $H = 10$ nm. In a first step, our numerical calculations were performed in the absence of the magnetic ($\gamma = 0$) and electric fields ($F = 0$). As we can see from Fig. 2, for a given value of the WL thickness L, the binding energy presents a qualitatively similar behavior to the case of a hydrogenic donor in others different geometrical QDs[52,53,61]. The binding energy growths up with decreasing the radius of the QD, reaches a maximum

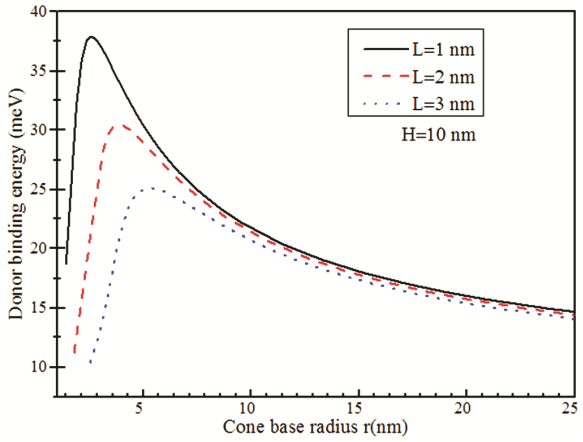

Fig. 2 – Binding energy of a donor impurity as a function of the cone base radius *r* for several values of the WL thickness L and with a fixed value of the *InAs* CQD height *H=10 nm*.

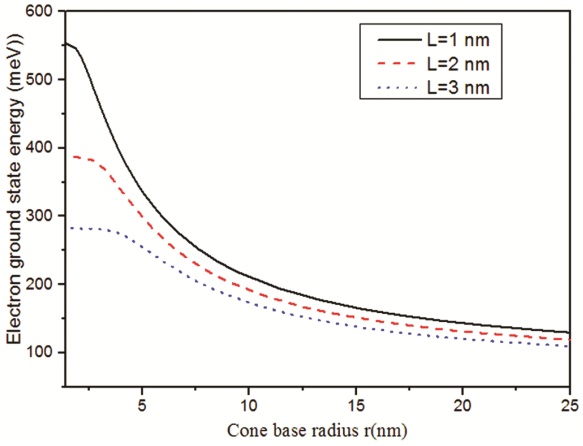

Fig. 3 – Variation of the ground state electron energy versus the cone base *r* radius for three values of the WL thickness L and with a fixed value of the *InAs* CQD height *H=10 nm*.

value and then decreasing sharply, which reflects that the electron wave function is firmly compressed in the InAs QD with decreasing the QD radius, when the QD radius decreases to a certain value, the kinetic energy of the confined electron rises greatly, the tunneling effects become dominant which in turn increases greatly the probability of the electron penetrating into the potential barrier GaAs by the uncertainly principle, therefore, the binding energy starts decreasing quickly. From both Figs. (2 & 3), it is seen that the effect of WL is negligible for higher values of the cone radius. While for small radii, a noticeable difference is observed indicating a quite significant contribution of the WL effects on the ground state energy and the donor binding energy. These results are in accordance with those regarding the effect of WL on the electronic states in InAs/GaAs QDs of pyramidal shaped[23] and dome-shaped[24]. Moreover, from Fig. 2, as the WL thickness increases, the binding energy decreases and particularly at small dot radius and its peak value is shifted to large values of the cone radius. The decreasing binding energy with the increasing WL is due to the increment of the QD confinement geometry. Figure 3 also shows that the WL changes the electron ground state energy significantly, more precisely, for very small dot radii, we observe that the electron ground state energy remains approximately constant for large values of the WL thickness (L = 3 nm). This is due to the localization of the electronic wave function mainly in the WL. This phenomenon is more noticeable as the WL thickness increases and it is also more significant for the case of the excited states[23,24]. Moreover, Fig. 3 shows also that the WL effect leads to a decrease of the ground state energy, which is consistent with the results obtained in Ref.[22-24].

Figure 4 shows the donor binding energy as a function of the electric field for different values of the magnetic field strength γ and with the following fixed structure parameters: H = 10 nm, r = 20 nm and L = 2 nm. For a given value of the effective field parameter γ, the binding energy increases as the electric field increases and this increment is important for positive electric field values. These results agree well with those obtained in Ref. [47] using a variational method in a GaAs/GaAlAs conical like QD with an infinite potential model. As the electric field increases from negative F = −100KV/cm to positive values F = 100KV/cm, the electronic wave function becomes more and more compressed since the size

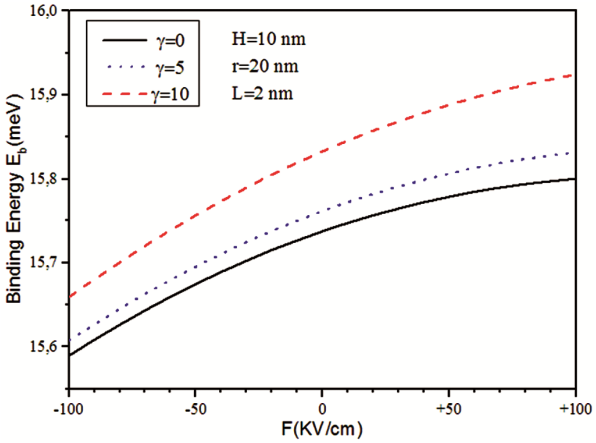

Fig. 4 – Variation of the donor binding energy as a function of the electric field for different values of the magnetic field strength y and with the following fixed structure parameters: H = 10 nm, r = 20 nm and L = 2 nm.

spatial region where the carriers are confined diminishes which leads to an enhancement of the binding energy. The values of the binding energy for positives values of the electric field are higher than those for negative values. This can be explained by the fact that from Eq. (1) a positive applied electric field (from 0 to 100KV/cm) implies that the electron is pushed to the -z direction, which is equivalent to an effective reduction of cone height[47] and hence the binding energy increases.

As expected, for a fixed value of the electric field, as the magnetic field increases, the binding energy increases. Furthermore, the effect of the magnetic field becomes more prominent for larger positive electric fields. The latter result is equivalent to saying that the binding energy is more sensitive to the electric field at higher magnetic fields. This is a consequence of the fact that in the strong magnetic field, the electron becomes more closely localized to the impurity and the effective separation between the confined electrons and the impurity center decreases, which leads to a strong magnetic confinement. Hence the combined effect of the strong magnetic confinement and the additional electric confinement coming from the application of an intense electric field leads to a higher localization of the electron wavefunctions inside the dot and this yields a strong enhancement of the binding energy.

Figure 5 illustrates the binding energy versus the magnetic field for different electric fields and with the following fixed structure parameters: H = 10 nm, r = 20 nm and L = 2 nm. It is observed that for every

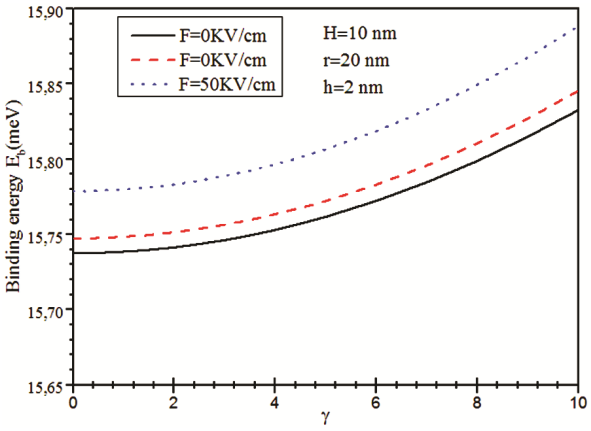

Fig. 5 – Variation of the ground state binding energy of a donor impurity with increasing magnetic field strength γ for different electric fields and with the following fixed structure parameters: H = 10 nm, r = 20 nm and L = 2 nm.

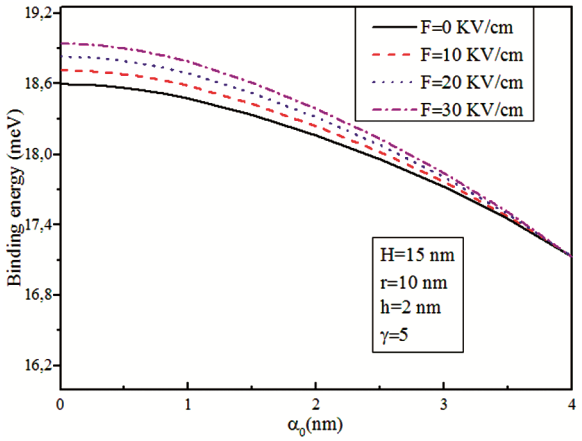

Fig. 6 – The ground state binding energy versus the laser-field amplitude α_0, for several values of the external electric field F with the following fixed structure parameters: H = 15 nm, r = 10 nm and L = 2 nm.and magnetic-field strength y = 5.

value of the electric field, the behavior of the binding energy versus the magnetic field strength is almost linear in the region of weak magnetic fields, in other words, the binding energy is relatively insensitive to the magnetic field effect for $\gamma < \gamma_c$, where γ_c is the critical magnetic field value at which the binding energy starts to increase and which depends on the electric field amplitude F. Since in the low magnetic field regime, the behavior of the binding energy is determined by the effect of the quantum confinement, the latter effect remains approximately invariable due to the fixed structure confinement goemetrical parameters H, r and L. While for very intense magnetic fields, the growth of the binding energy is more pronounced. This can be understood as follows. At high magnetic fields, magnetic confinement becomes stronger and the confining potential V_c is considered as a small perturbation on the magnetic energy and therefore, the binding energies very weakly depend on the dimensions of the structure. As mentioned previously, for a fixed value of γ, the binding energy increases as the amplitude F of an applied static electric field enlarges and the critical magnetic field value γ_c decreases.

In Fig. 6, we depict the donor binding energy of the ground state as a function of the laser-field amplitude α_0, for several values of the external electric field F with the following fixed structure parameters: H = 15 nm, r = 10 nm and L = 2 nm and magnetic-field strength γ = 5. At zero electric field, the behavior of this figure is the result of the coupling and competition of the laser–dressed Coulomb potential with the barrier confining potential V_c.

As seen in this figure, for a fixed value of F and for weakly values α_0, the dependency of the binding energy on the laser radiation is very small. But for further large values of α_0, the expectation value of the effective spatial separation along the z-direction between the electron and dressed Coulomb center is enhanced due the spatial extension of the electron probability density[38,62]. The spread of the electron wave function over a larger region within the structure weakens the Coulomb interaction and the impurity binding energy decreases drastically. The same results are found in others systems like cylindrical QDs[62] and quantum well wires[63]. At the same time as we expected, Fig. 6 shows that the binding energy increases with electric field F up to the value of $\alpha_0 \cong 3$ nm, since electric field gives an additional lateral confinement of the charge carrier and the probability of finding the electron in the InAs QD increases with F, resulting in higher binding energy. But for large enough laser field values, the electronic orbital is more weakly localized around the impurity, a weaker dependence of the Coulomb potential with α_0 is found, the geometric confinement becomes therefore weak and the donor binding energy does not depend on the electric field, reflecting the three-dimensional character of the wave function of the particles after they penetrate into the classically forbidden region. The behavior of the binding energy as a function of the laser field in the presence of a uniform electric field is similar to that exhibited in other hetero structures like quantum well structure[64].

Figure 7 shows the behavior of the binding energy for a donor impurity in a InAs/GaAs CQD as a

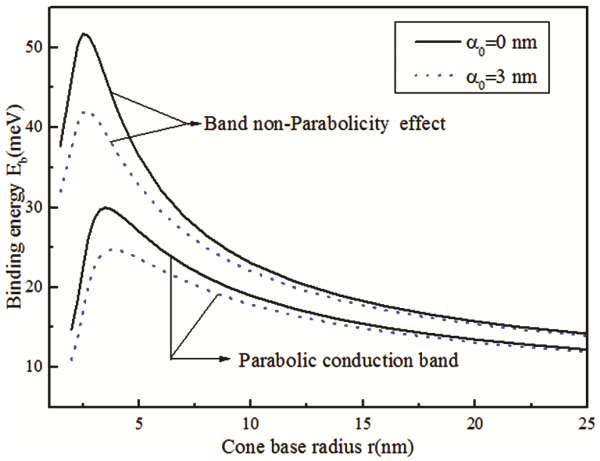

Fig. 7 – The binding energy of a donor impurity in a $InAs/GaAs$ CQD as a function of the cone base radius for two values of the laser-field amplitude $\alpha_0 = 0$ and $\alpha_0 = 3$ nm and with and without the conduction band-edge non-parabolicity effect.

function of the cone base radius for two values of the laser-field amplitude $\alpha_0 = 0$ and $\alpha_0 = 3$ nm with and without the conduction band-edge non-parabolicity effect. For a fixed value of α_0, a quite noticeable deviation between the curves in the presence and absence of the non-parabolicity effect is produced for small CQD radii. In other words, we can say that the contribution of the non-parabolicity effect alters considerably the donor binding energy in the strong spatial confinement regime, more precisely, the inclusion of the band non-parabolicity effect reduces the tunneling effect across the barrier and leads to more binding energy. These results prove that the energy dependent effective mass Eq. (8) gives quite accurate results than the quadratic dispersion relation (parabolic approximation) especially for relatively small CQD geometries parameters. While in the low confinement regime, the effect of the conduction band non-parabolicity becomes gradually smaller as the value of the cone radius increases. Our findings are in good agreement with the previous calculations for other low dimensional structures[53,61,65].

For both parabolic and non-parabolic band approximations, it can be seen that the effect of the laser dressing is strongly dependent on the CQD radius. The results indicate that the effect of laser field is more appreciable for narrow dots only in perfect agreement with the quasi-two and quasi-one dimensional case[63,64]. For large CQD radii, the discrepancy between the two curves $\alpha_0 = 0$ and $\alpha_0 = 3$ nm is too small and the effect of the laser dressing parameter α_0 on the binding energy is negligible. Since for large enough dot radius values, the geometric confinement becomes weak and the donor binding energy does not depend on the laser field and tend to the saturation regime for both values of α_0. Our results agree well with those obtained by several authors in different shapes of low dimensional semiconductors[63,66,67].

This figure reveals again that the influence of high-frequency laser increases with the non-parabolicity effect in the regime of small QD radius. This is due to the increment of the spatial localization of the electron with the non-prabolicty effect, which in turn increases the quantum confinement and leads to an enhancement of the binding energy. This effect has not been shown by H. El Ghazi[67] since his calculations on the binding energy in the absence and presence of the non-parabolicity effect have been carried out for $\alpha_0 = 0$.

We also observe that the peak position of the donor binding energy moves slightly toward the smaller radius as both the non-parabolicity and the laser dressing parameter effects are introduced[53,67]. This shift to narrow dots can be explained by the shrinkage of the spatial extent of the wavefunction under the both effects.

4 Conclusions

We have studied the effects of WL and conduction band non-parabolicity combined with the external perturbations such as the applied magnetic and electric fields as well as the high-frequency laser field on the ground state energy and binding energy of a donor impurity confined in a InAs CQD embedded in a GaAs matrix The calculations were done in the effective mass and non-parabolic band approximations using the FEM. The study considers also the variation of the donor binding energy as a function of the dimensions of the CQD such as the cone radius. It is found that the influence of the WL, the non-parabolicity and the high-frequency laser field are more significant in the regime of small QD radius. The binding energy increases with the increasing magnetic fields strengths, decreases drastically for large values of the laser dressing parameter α_0 and it is more sensitive to the electric field at higher magnetic fields.

References

1 Mowbray D J & Skolnick M S, *J Phys D: Appl Phys*, 38 (2005) 2059.
2 Bimberg D, *J Phys D: Appl Phys*, 38 (2005) 2055.

3 Chen S, Tang M, Jiang Q, *ACS Photonics*, 1 (2014) 638.
4 Kapteyn C M A, Heinrichsdorff F, Stier O, Heitz R, Grundmann M, Zakharov N D, Bimberg D & Werner P, *Phys Rev B*, 60 (1999) 14265.
5 Michler P, Single semiconductor quantum dots, Springer, Heidelberg, 2009.
6 Majid M A, Childs D T D, Kennedy K, Airey R, Hogg R A, Clarke E, Spencer P & Murray R O, *Appl Phys Lett*, 99 (2011) 051101.
7 7 Shields A J, O'Sullivan M P, Farrer I, Ritchie D A, Hogg R A, Leadbeater M L, Norman C E & Pepper M, *Appl Phys Lett*, 76 (2000) 3673.
8 Ledentsov N N, *Semicond Sci Technol*, 26 (2011) 014001.
9 Moreau E, Robert I, Gérard J M, Abram I, Manin L & Thierry-Mieg V, *Appl Phys Lett*, 79 (2001) 2865.
10 Hasegawa Y, Kiyama H, Xue Q K & Sakurai T, *Appl Phys Lett*, 72 (1998) 2265.
11 Baskaran A & Smereka P, *J Appl Phys*, 111 (2012) 044321.
12 Marzin J Y & Bastard G, *Solid State Commun*, 92 (1994) 437.
13 Pryor C, *Phys Rev B*, 57 (1998) 7190.
14 Ngo C Y, Yoon S F, Fan W J & Chua S J, *Phy Rev B*, 74 (2006) 245331.
15 Safarpour G, Barati M, Vahdani M, *Physica E*, 44 (2011) 728.
16 Liang G, Yong-Chun S, Jing-Jun X & Zhan-Guo W, *Superlattices Microstruct*, 61 (2013) 81.
17 Oshima R, Kurihara N, Shigekawa H & Okada Y, *Phys E*, 21 (2004) 414.
18 Seravalli L, Bocchi C, Trevisi G & Frigeri P, *J Appl Phys*, 108 (2010) 114313.
19 Lee S, Lazarenkova O L, Allmen P von, Oyafuso F & Klimeck G, *Phys Rev B*, 70 (2004) 125307.
20 Grundmann M, Stier O & Bimberg D, *Phys Rev B*, 52 (1995) 11969.
21 Melnik R V N & Willatzen M, Nanotechnology, 15 (2004) 1.
22 Zhao Q, Mei T, Zhang D & Kurniawan O, *Opt Quant Electron*, 42 (2011) 705.
23 Sabaeian M & Khaledi-Nasab A, *Appl Opt*, 51 (2012) 4176.
24 Shahzadeh M & Sabaeian M, *AIP Advances*, 4 (2014) 067113.
25 Cusack M A, Briddon P R & Jaros M, *Physica B*, 253 (1998) 10.
26 Goser K, Glosekotter P & Dienstuhl J, *Nanoelectron Nanosyst*, Springer, New York, 2004.
27 Weisbuch C & Vinter B, Quantum Semiconductor Structures, Academic, Orsay, France, 1991.
28 Duque C A, Montes A, Morales A L & Porras-Montenegro N, *J Phys Condens Matter*, 9 (1997) 5977.
29 Barseghyan M G, Mora-Ramos M E & Duque C A, *Eur Phys J B*, 84 (2011) 265.
30 Ledentsov N N, Ustinov V M, Shchukin V A, Kop'Ev P S, Alferov Z I & Bimberg D, *Semicond*, 32 (1998) 343.
31 Lu M, Yang X J, Perry S S & Rabalais J W, *Appl Phys Lett*, 80 (2002) 2096.
32 Bahramiyan H & Khordad R*, Int J Mod Phys B*, 28 (2014) 1450053.
33 Tiriba G C, Niculescu E C & Burileanu L M, Superlattices Microstruct, 75 (2014) 749.
34 Khordad R & Bahramiyan H, *Commun Theor Phys*, 62 (2014) 283.
35 Niculescu E, Tiriba G & Spandonide A, *UPB Sci Bull Ser A*, 77 (2015) 1223.
36 Aderras L, Bah A, Feddi E, Dujardin F & Duque C A, *Physica E*, 89 (2017) 119.
37 Ganichev S D & Prettl W, Intense Terahertz Excitation of Semiconductors, Oxford University Press, Oxford, 2006.
38 Niculescu E C, *Physica E*, 63 (2014) 105.
39 Hayrapetyan D B, Kazaryan E M & Sarkisyan H A, *Opt Commun*, 371 (2016) 138.
40 Huggenberger A, Schneider C, Drescher C, Heckelmann S, Heindel T, Reitzenstein S, Kamp M, Hofling S, Worschech L & Forchel A, *J Cryst Growth*, 323 (2011) 194.
41 Pickering S, Kshirsagar A, Ruzyllo J & Xu J, *Optoelectron Rev*, 20 (2012) 148
42 Yamaguchi M, Asano T & Noda S, *Opt Expr*, 16 (2008) 18067.
43 Vorobiev Y V, Torchynska T V & Horley P P, *Physica E*, 51 (2013) 42.
44 Khordad R & Bahramiyan H, *Opt Spectrosc*, 117 (2014) 447.
45 Kazaryan E M, Petrosyan L S, Shahnazaryan V A & Sarkisyan H A, *Commun Theor Phys*, 63 (2015) 255.
46 Baghdasaryan D A, Hayrapetyana D B, Sarkisyan H A, Kazaryan E M & Medvids A, *J Contemp Phys*, 52 (2017) 129.
47 Iqraoun E, Sali A, Rezzouk A, Feddi E, Dujardin F, Mora-Ramos M E & Duque C A, *Philos Mag*, 97 (2017) 1445.
48 Gil-Corrales A, Morales A L, Restrepo R L, Mora-Ramos M E & Duque C A, *Physica B: Condensed Matter*, 507 (2017) 76.
49 Khordad R & Bahramiyan H, *Physica E*, 66 (2015) 107.
50 Khordad R & Bahramiyan H*, Eur Phys J Appl Phys*, 67 (2014) 20402.
51 Satori H & Sali A, *Physica E*, 48 (2013) 171.
52 Sali A & Satori H, *Superlattices Microstruct*, 69 (2014) 38.
53 Sali A, Kharbach J, Rezzouk A & Ouazzani J M, *Superlattices Microstruct*, 104 (2017) 93.
54 Kotera N & Tanaka K, *Physica E*, 32 (2006) 199.
55 Kwon H Y, Woo J T, Lee D U, Kim T W & Park Y J, Solid State Commun, 149 (2009) 52.
56 Ehlotzky F, *Phys Lett A* , 126 (1988) 524.
57 Fanyao O & Fonseca A L A, Nunes O A C, *Phys Rev B*, 54 (1996) 16405.
58 Li S & Xia J B, *J Appl Phys*, 89 (2001) 3434.
59 Colombelli R, Piazza V, Badolato A, Lazzarino M & Beltram F, *Appl Phys Lett*, 76 (2000) 1146.
60 Madelung O, Schultz M & Weiss H, Physics of Group IV Elements and III-V Compounds, Landolt-Börnstein, Group III, Springer-Verlag, Berlin, 17 (1982).
61 Sivakami A & Mahendran M, *Physica B*, 405 (2010) 1403.
62 Duque C A, Kasapoglu E, Sakiroglu S, Sari H & Sökmen I, *Appl Surface Sci*, 256 (2010) 7406.
63 Niculescu E C & Burileanu L M*, J Optoelectron Adv Mater*, 9 (2007) 2713.
64 John Peter A, *Phys Lett A*, 374 (2010) 2170.
65 Aktaş Ş, Okan S E, Erdoğan I, Akba Ş H & Tomak M, *Superlattices Microstruct*, 28 (2000) 165.
66 Lopez F E, *J Phys D: Appl Phys*, 42 (2009) 115304.
67 El Ghazi H, *Int J Mod Phys B*, 29 (2015) 1450246-1-8.